Published OnlineFirst September 8, 2009; DOI: 10.1158/0008-5472.CAN-09-1140

Epigenetic Loss of Mucosa-Associated Lymphoid Tissue 1 Expression in Patients with Oral Carcinomas

Tadashige Chiba,[1] Genta Maeda,[1] Shuichi Kawashiri,[2] Koroku Kato,[2] and Kazushi Imai[1]

[1]Department of Biochemistry, School of Life Dentistry at Tokyo, The Nippon Dental University, Chiyoda-ku, Tokyo, Japan and [2]Department of Oral Surgery, School of Medicine, Kanazawa University, Kanazawa, Ishikawa, Japan

Abstract

Mucosa-associated lymphoid tissue 1 (MALT1), which is located in a genomic region that encodes unknown tumor suppressor gene(s), activates nuclear factor-κB in lymphocyte lineages. However, its expression and role in the pathology of malignant tumors of epithelial origin is not known. In the present study, we examined MALT1 expression and its implications for the pathology of oral carcinomas. Immunostaining localized MALT1 in the nucleus of normal oral epithelial cells, but the expression was absent in 45.0% of carcinomas (49 of 109 cases) especially at the invasive front. The loss of expression was correlated with tumor recurrence ($P = 0.007$) and poor patient survival ($P < 0.001$), and it was an independent prognostic determinant ($P < 0.001$). MALT1-negative carcinomas exhibited microsatellite instability at the *MALT1* locus and a specific cytosine methylation positioned at −256 from the gene, and the expression was recovered by demethylation treatment. In contrast to lymphocyte lineages, carcinoma cells showed MALT1 located at the nucleus independent of its domain structures, and its loss of expression induced the epithelial-mesenchymal transition. These results show that MALT1 is expressed in the nucleus of oral epithelial cells and that its expression is epigenetically inactivated during tumor progression, suggesting that the detection of MALT1 expression is a useful predictive and prognostic determinant in the clinical management of oral carcinomas. [Cancer Res 2009;69(18):7216–23]

Introduction

Worldwide, the annual incidence of new cases of oral carcinoma is estimated at 350,000 to 400,000 and is predicted to increase in the next few decades. In the United States, 30,000 new oral carcinoma cases are diagnosed annually and 11,000 people die of the disease each year. Notably, the 5-year survival rate of patients has not been sufficiently improved. Regardless of the therapeutic approaches used and the location and stage of the diseases, >50% of patients experience a relapse (1). Treatment failure can be attributed to multiple factors, but no reliable molecular marker is currently available. The tailoring of individual treatment strategies to aggressively treat those carcinomas at greatest risk of causing patient death would likely improve long-term survival. There is an urgent need to identify characteristics of the primary tumor that might predict aggressive tumors.

Tumor suppressor gene inactivation has been implicated in the initiation and development of carcinomas. In oral carcinomas, expression of the tumor suppressors p53, $p14^{ARF}$, $p16^{INK4a}$, FHIT, and RSSF1 was frequently inactivated in the early stage of carcinogenesis (1). Allelic imbalance at chromosome locus 18q is associated with progression and poor patient survival of head and neck carcinomas (2, 3), and genetic abnormalities at 18q21 are observed in carcinomas of the oral cavity (National Center for Biotechnology Information Entrez Cancer Chromosome Database[3]) and others (4–6). Although one tumor suppressor gene, *deleted in colorectal carcinoma* (*DCC*), exists at 18q21.1, recent investigations suggest the presence of additional tumor suppressors at 18q21.31 (7, 8). Among the genes encoded within the locus, *mucosa-associated lymphoid tissue 1* (*MALT1*) activates nuclear factor-κB (NF-κB) and is involved in tumorgenesis in lymphocyte lineages. MALT1 is made up of three types of domain: a death domain at the NH_2 terminus, Ig-like domains, and a caspase-like domain at the COOH terminus. The T-cell receptor or B-cell receptor antigen signals oligomerize MALT1 with B-cell lymphoma 10 (BCL10) and caspase recruitment domain membrane-associated guanylate kinase protein 1 into a CBM complex. MALT1 interacts with BCL10 through its Ig-like domains, and it induces IκB-kinase (IKK) catalytic activity by its caspase-like domain, resulting in NF-κB activation (9). Although *MALT1* is expressed not only in lymphocyte lineages but also in a variety of tissues (10), its role in the pathology of carcinomas of epithelial origin is not known. In the present study, we examined the expression of MALT1 in oral carcinomas and the mechanisms responsible for its inactivation.

Materials and Methods

Cell lines, plasmids, and short interfering RNA. Oral carcinoma cells lines were used as previously described (11, 12). The full-length wild-type *MALT1* (*wtMALT1*; 1-824 amino acids), the NH_2 terminus (1–332 amino acids) of *MALT1* (*nMALT1*), and the NH_2 terminus–deleted dominant-negative form (333–824 amino acids) of *MALT1* (*ΔMALT1*) cDNAs (13) were cloned into pCMV with a FLAG-tag (pCMV-Tag 2A; Stratagene) or pcDNA4-HisMaxB (Invitrogen). An oral carcinoma cell line, HSC2, was transfected with the plasmids, and cells stably expressing *wtMALT1* ($_{wtMALT1}$HSC2 cells), *ΔMALT1* ($_{\Delta MALT1}$HSC2 cells), or vector alone ($_{mock}$HSC2 cells) were selected with 100 μg/mL of G418 (14).

Antibodies. A rabbit polyclonal anti-MALT1 antibody against A^{26}GATLNRLREPLLRR^{40} was purified by an affinity column coupled with synthetic peptides. The antibody preparations were screened by ELISA using the peptide. Antibodies specific to histone H3, IKKα (Cell Signaling), involucrin, β-actin, FLAG (Sigma), cytokeratin 10 (Progen Bioteknik GmbH), or E-cadherin (R&D Systems) were used for immunoblotting.

Patient population. A total of 109 individual oral squamous cell carcinomas were taken at Kanazawa University Hospital during incisional or excisional biopsy. The median age of the study patients was 64 y (range, 37–93 y) at the time of diagnosis. Patients underwent surgery ($n = 93$) or radiation and surgery ($n = 16$). The details of the pretreatment clinical and

Note: Supplementary data for this article are available at Cancer Research Online (http://cancerres.aacrjournals.org/).

Requests for reprints: Kazushi Imai, Nippon Dental University, 1-9-20 Fujimi, Chiyoda-ku, Tokyo 102-8159, Japan. Phone: 81-3-3261-8857; Fax: 81-3-3261-8875; E-mail: kimai@tky.ndu.ac.jp.

doi:10.1158/0008-5472.CAN-09-1140

[3] http://www.ncbi.nlm.nih.gov/sites/entrez?db=cancerchromosomes

Published OnlineFirst September 8, 2009; DOI: 10.1158/0008-5472.CAN-09-1140

Table 1. Clinicopathologic parameters and MALT1 expression in 109 primary oral carcinomas

Parameters	MALT1 staining		
	n	Mean ± SD*	*P*
Sex			
Female	47	1.60 ± 1.17	
Male	62	1.50 ± 1.16	0.671†
T stage‡			
T1	27	1.89 ± 1.09	
T2	52	1.58 ± 1.21	
T3	10	1.20 ± 1.03	
T4	20	1.15 ± 1.09	0.130§
N stage‡			
N0	71	1.69 ± 1.17	
N1	24	1.38 ± 1.01	
N2	13	1.08 ± 1.32	
N3	1	1.00 ± 0.00	0.267§
Clinical stage‡			
Stage 1	25	2.04 ± 1.02	
Stage 2	38	1.61 ± 1.24	
Stage 3	19	1.37 ± 1.01	
Stage 4	27	1.11 ± 1.12	0.029§
Histologic differentiation			
Well	51	1.90 ± 1.23	
Moderate	39	1.44 ± 1.14	
Poor	19	0.79 ± 1.18	0.001§

*MALT1 staining was graded by the ratio of immunoreactive carcinoma cells, where 0 is no staining, 1+ is ≤10%, 2+ is 11–40%, and 3+ is ≥41% staining of cells.

† Probability of statistical difference was analyzed by Mann-Whitney *U* test.

‡ Patients were categorized by tumor size (T stage) and clinical stage according to the UICC WHO grading system and by the stage of lymph node metastasis (N stage).

§ Probability of statistical difference was analyzed by analysis of covariance.

pathologic characteristics are summarized in Table 1. Histologic grading and staging were assessed according to the 1987 International Union Against Cancer (UICC) tumor-node-metastases classification (15). Follow-up data were retrieved from medical records and confirmed by direct interviews with the patients' oral surgeons. Carcinoma-related deaths were identified by the presence of prior metastasis of oral carcinoma during the survival analysis. Normal gingival tissues were obtained from five carcinoma-free patients undergoing dental surgeries. All tissues were obtained with the written consent of the patient and with approval by the institutional review boards of Kanazawa University and Nippon Dental University.

Immunostaining. Unstained formalin-fixed and paraffin-embedded carcinoma (n = 109) and normal gingival tissue sections (n = 5) were incubated with anti-MALT1 antibody followed by biotinylated anti-rabbit IgG. After treatment with avidin-biotin complexes, the color was developed with 3,3′-diaminobenzidine tetrahydrochloride. The immunostaining of MALT1 was graded by measuring the ratio of immunoreactive carcinoma cells in at least 3,000 cells in randomly selected areas of each specimen, where 0 is no staining, 1+ is ≤10%, 2+ is 11% to 40%, and 3+ is >40% staining of the cells. The grading were blinded as to the clinicopathologic parameters and verified by two independent observers (TC and KI). To clarify the specificity of the staining, sections were reacted with nonimmune rabbit IgG instead of primary antibody.

Reverse transcription-PCR and quantitative real-time PCR. Total RNA was extracted from carcinoma tissues (n = 7) and normal gingival tissues (n = 3), which were snap-frozen in TRIzol reagent (Invitrogen) and reverse transcribed to a single-stranded cDNA with random hexamer (Invitrogen), followed by reverse transcription-PCR (RT-PCR) by running 30 cycles (94°C for 40 s; 54°C for 40 s for *GAPDH*, and 56°C for 40 s for *MALT1*; 72°C for 1 min) using gene-specific primer sets for *MALT1* and *GAPDH* for *MALT1* (Supplementary Table S1). For the quantitative analysis of *MALT1* expression, carcinoma cells cultured for 4 d in the presence or absence of 5 μmol/L 5-aza-2-deoxycytidine (5-aza) were harvested for isolation of total RNA. The cDNA reverse transcribed from RNA by MultiScribe Reverse Transcriptase (Applied Biosystems) was subjected to real-time PCR using the StepOne Real-Time PCR system (Applied Biosystems) in triplicate. PCR conditions were 95°C for 20 s followed by 40 cycles of 95°C for 1 s and 60°C for 20 s. The *MALT1*-specific TaqMan probe was synthesized from sequence at the boundary of exons 15 and 16 (Assay-on-Demand Gene Expression system, Hs0112005-m1; Applied Biosystems). Expression levels were normalized against *β-actin* (TaqMan Endogenous Control Human *ACTB*; Applied Biosystems). Levels of gene expression ($2^{-\Delta\Delta Ct}$) were determined by the standard curve method (12).

DNA extraction. Microdissection and DNA extraction from 8-μm-thick paraffin-embedded tissue sections (n = 47) were carried out using a laser capture microdissection apparatus (Leica Microsystems). Tumor cells and adjacent normal cells were separately microdissected, and genomic DNA was extracted by a standard protocol (16) and quantified by a spectrophotometer.

Microsatellite markers and PCR. Genomic DNA was subjected to microsatellite analysis using an established marker (D18S1117) positioned at 151.2 kb downstream of *MALT1*. Because there are no established microsatellite markers within the *MALT1* locus, three intragenic markers were designed (*MALT1e1* at intron 2, *MALT1e2* at intron 4, and *MALT1e3* at intron 13) spanning (CA)n, (TG)n, and (CA)n, respectively (Supplementary Table S1). Genomic DNA (20 ng) was amplified in a volume of 20 μL by 35 cycles of touchdown PCR (denaturation for 45 s at 94°C, annealing for 1 min and elongation for 1 min at 72°C). The annealing temperature began at 66°C and was lowered 1°C per cycle. About 15 μL of the amplified products were electrophoresed through acrylamide gels stained by Vistra Green (Amersham Bioscience) and were scanned by a Typhoon 9410 Image Analyzer (Amersham Bioscience).

Genetic instability and allelic imbalance. The allelic profile of each carcinoma was initially scored for microsatellite instability (MSI) according to a criterion for alterations in allelic length (17). Sometimes it was not possible to distinguish between MSI and the loss of heterozygosity (LOH), especially in cases with intimately close heterozygous allelic bands. A signal reduction in one of two alleles might result not only from allelic loss but also from allelic shift attributable to comigration with an adjacent allele. Thus, if multiple bands or novel allelic bands that were not observed in normal DNA were found in the corresponding tumor DNA, they were interpreted as MSI. The LOH of tumor DNA was scored as relative allelic ratio, which was calculated by dividing the tumor allelic ratio by the normal allelic ratio (18).

Bisulfite-modified sequencing of *MALT1* promoter region. The 5′ proximal promoter region of *MALT1* was analyzed on the computer program CpG Island Finder[4] to find CpG islands. Genomic DNA isolated from carcinoma cell lines was treated with sodium bisulfite (18) and applied for direct sequencing using a PCR primer set from −48 to −341 (Supplementary Table S1).

Methylation-specific PCR. Genomic DNA isolated from carcinoma cell lines or carcinoma cells of tissue sections was modified by sodium bisulfite treatment. Methylation-specific PCR (MSP) was carried out on the modified DNA to detect cytosine methylation positioned at −256 (from the transcription start site) using primer sets recognizing methylated $^{-256}$C (methyl primers) and unmethylated $^{-256}$C (unmethyl primers), which amplify the *MALT1* CpG island from −139 to −240 (Supplementary Table S1). PCR amplification using AccuPrime Taq DNA polymerase (Invitrogen) was performed by running 48 cycles as follows: denaturing for 30 s at 94°C, annealing for 30 s (at 59°C for first 4 cycles, 57°C for next 4 cycles, and 55°C

[4] http://cpgislands.usc.edu/

Published OnlineFirst September 8, 2009; DOI: 10.1158/0008-5472.CAN-09-1140

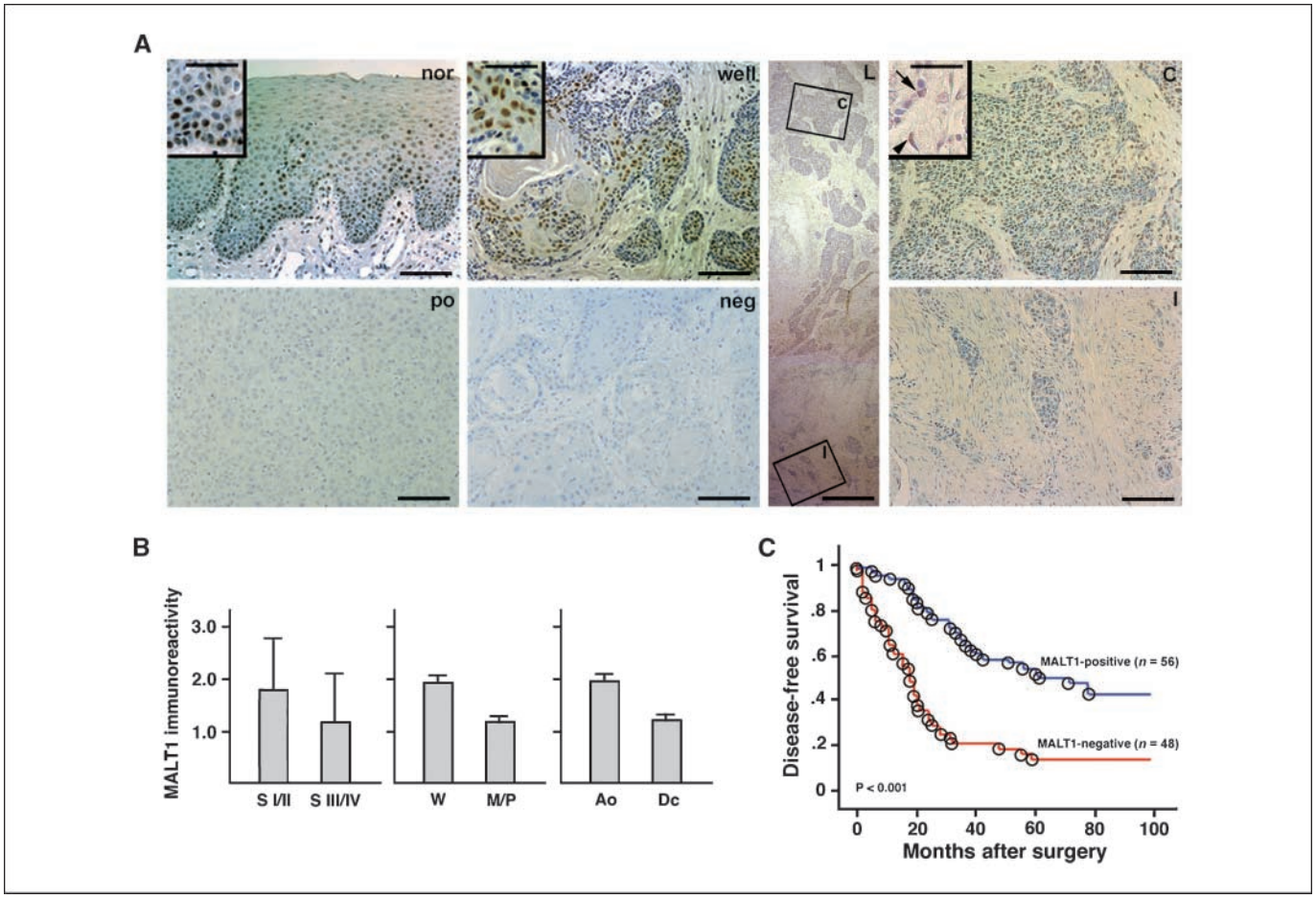

Figure 1. Expression of MALT1 and patient prognosis. *A,* MALT1 immunostaining of normal gingiva (*nor*), well-differentiated (*well*) and poorly differentiated (*po*) carcinomas, and a negative control using nonimmune IgG instead of primary antibody (*neg*). *Insets,* high-power views of the staining. *L,* a low-power view of the staining. A high-power view of the staining at the center or invasive front is shown in *c* (*inset c* in *L*) or *I* (*inset I* in *L*), respectively. An arrowhead shows cytoplasmic staining in a fibroblast and an arrow shows nuclear staining in a carcinoma cell in an inset in *c*. *Scale bars,* 125 μm (*L*), 50 μm (*nor, well, po, neg, c*, and *I*), and 15 μm (*insets*). *B,* MALT1 immunoreactivity of carcinoma cells was compared between groups with clinical stages (*left: S I/II,* stages I and II; *S III/IV,* stages III and IV: $P = 0.012$), tumor differentiation (*center: W,* well-differentiated tumor; *M/P,* moderately and poorly differentiated tumors; $P = 0.002$), or tumor recurrence (*right: Ao,* cases free of tumor recurrence; *Dc,* cases that died of tumor recurrence; $P = 0.007$). *Columns,* mean; *bars,* SD. *C,* long-term survival of MALT1-negative and MALT1-positive patients ($n = 104$; $P < 0.001$; log-rank test).

for the rest), and extension for 30 s at 68°C (19). Distilled water, instead of sodium bisulfite, was used as a negative control.

Statistical analyses. For the analysis of probabilities of postoperative survival of patients ($n = 104$), except those who died of other diseases, we divided patients into two groups, a negative group (grade 0 and 1) and a positive group (grade 2 and 3), using the Kaplan-Meier method and analyzing the statistical difference by the log-rank test. The postoperative period was measured from the date of surgery to the date of the last follow-up or death. The influence of clinicopathologic parameters and MALT1 immunoreactivity on patient survival was analyzed by the multivariate Cox proportional hazards method, which included variables of pathologic stage, patient age, and MALT1 immunostaining status. The Mann-Whitney *U* test and analysis of covariance were used for all other comparisons. Differences with *P* values of <0.05 were considered statistically significant.

Results

Loss of MALT1 expression in progressive carcinomas. To investigate the expression and localization of MALT1, we generated an antibody specific for the NH_2 terminus of MALT1 (Supplementary Fig. S1). MALT1 localizes in the nuclei of basal and suprabasal cells of normal gingival epithelium, but not in their cytoplasm (Fig. 1*A*). We immunostained 109 individual primary oral carcinomas and graded them into four categories (0–3+) according to the percentage of carcinoma cells with nuclear staining. MALT1 was not detected in 45.0% of the cases, and in the remainder, its level of expression declined in conjunction with the dedifferentiation of carcinomas ($P = 0.001$) and the progression of clinical stage ($P = 0.029$; Table 1). In contrast to the central area of carcinoma tissues, carcinoma cells at the invasive front, where they proliferate downward into the connective tissue and exhibit epithelial-mesenchymal transition (EMT; ref. 12), showed weaker staining (Fig. 1*A*). Specificity of the staining was confirmed by the cytoplasmic staining in fibroblasts (Fig. 1*A*, an inset of *c*), wherein MALT1 acts as a NF-κB–activating signaling molecule (20). MALT1 staining was decreased in groups of advanced clinical stage (stage 1 and 2 versus stage 3 and 4, 1.78 ± 1.17 versus 1.22 ± 1.11; mean ± SD; $P = 0.012$) and less (moderately and poorly) differentiated carcinomas (well-differentiated versus less differentiated carcinomas, 1.90 ± 0.16 versus 1.22 ± 0.15; $P = 0.002$; Fig. 1*B*).

A total of 69 of 104 patients (excluding patients who died of other diseases) who died of disease recurrence (*Dc*) had decreased MALT1 staining (1.29 ± 1.14), compared with patients who did not

Published OnlineFirst September 8, 2009; DOI: 10.1158/0008-5472.CAN-09-1140

Table 2. Contribution of clinicopathologic risk factors to disease-specific survival of oral carcinoma patients (n = 104)

Parameters	Risk ratio	95% CI*	P †
Age (≤50 y vs >50 y)	0.903	0.515–1.584	0.723
T stage (T1/2 vs T3/4)	1.531	0.447–2.473	0.082
Lymph node status (N− vs N+) ‡	1.346	0.772–2.345	0.295
Clinical stage (stage 1/2 vs stage 3/4)	1.032	0.525–2.030	0.927
Histologic differentiation (well- vs moderately/poorly differentiated)	1.638	1.124–2.388	0.010
MALT1 staining (negative vs positive) §	1.809	1.220–2.683	<0.001

*Confidence interval.
†Cox proportional hazards method.
‡N−, cases without lymph node metastasis; N+, cases with metastasis.
§Negative, groups 0 and 1; positive, groups 3 and 4.

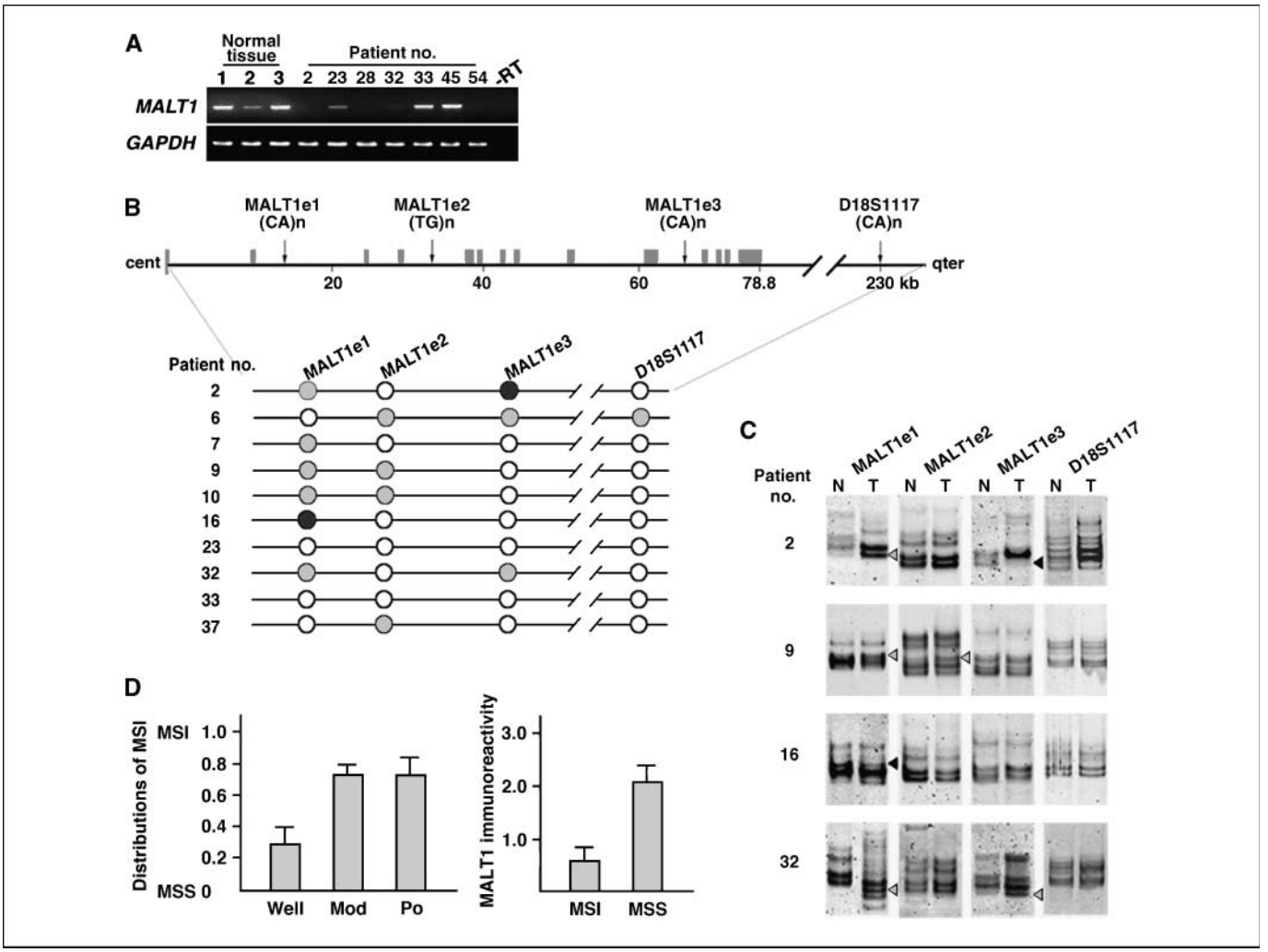

Figure 2. MSI at the *MALT1* locus. *A,* expression of MALT1 mRNA in normal gingiva and carcinoma tissues. MALT1 expression in normal gingival tissues (*normal tissues 1–3*) and carcinoma tissues (*patient no. 2–54*) was examined by RT-PCR. *−RT,* negative control without reverse transcription of RNA isolated from a normal tissue number 3 sample. *B,* MSI and LOH patterns in representative carcinoma patients. Retained microsatellite markers (*white*), LOH (*black*), and MSI (*gray*) are shown. *C,* representative gel electrophoresis of microsatellite PCR. *Gray arrowheads,* MSI; *black arrowheads,* allelic imbalance. Genomic DNA of carcinoma cells (*T*) and distant normal cells (*N*) were independently isolated from the same tissue section in each patient by laser-captured microdissection. *D,* distributions of MSI at the *MALT1* locus and tumor differentiation and MALT1 staining. The presence of MSI was determined as 1 and microsatellite stability (*MSS*) as 0. *Well,* well-differentiated tumors; *Mod,* moderately differentiated tumors; and *Po,* poorly differentiated tumors (*left*; P = 0.041). MALT1 immunoreactivity of carcinoma cells was compared with genetic instability (*right*; P < 0.001). *Columns,* mean; *bars,* SD.

Published OnlineFirst September 8, 2009; DOI: 10.1158/0008-5472.CAN-09-1140

have tumor recurrence (*Ao*) during the follow-up period (1.91 ± 1.10; $P = 0.007$; Fig. 1*B*). The MALT1-negative group (grades 0 and 1) exhibited significantly lower disease-specific survival than the positive group (grades 2 and 3; $P < 0.001$, log-rank test; Fig. 1*C*). The progression of T stage and clinical stage, the presence of lymph node metastasis, and carcinoma dedifferentiation also lowered survival (Supplementary Fig. S2). Univariate risk factor analysis found that the MALT1-negative group increased the risk ratio of death (2.734; $P < 0.001$; Supplementary Table S2). A multivariate model was then used to adjust for the potential influence of confounding factors. MALT1 staining was a significant predictor of disease-specific death independent from other risk factors ($P < 0.001$; Table 2). Loss of MALT1 staining (grades 0 and 1) reduced patient survival with a hazard ratio of 1.809 and a confidence interval ranging from 1.220 to 2.683. These data indicate a close association of loss of MALT1 expression with oral carcinoma progression.

Genetic instability and promoter methylation. *MALT1* gene expression was detected by RT-PCR in all normal gingival tissues but was frequently undetectable in carcinoma tissues (Fig. 2*A*). The absence of expression did not seem to result from the presence of a premature termination codon, because the expression pattern was identical when a primer set for exon 1 was used (data not shown). Then, allelic imbalance and MSI at the *MALT1* locus in 47 randomly selected carcinomas was analyzed. In 51.1% of these carcinomas, the electrophoretic mobility of the band was shifted relative to their normal counterparts, reflecting changes of dinucleotide repeat number (Fig. 2*B* and *C*). Fourteen cases exhibited two or three MSI (29.8%), and 10 cases showed one MSI (21.3%). Allelic loss was limited in four cases, and homozygous deletion in one. The other 18 cases (38.3%) exhibited microsatellite stability. The frequency of MSI increased in less differentiated carcinomas (71.4%; 20 of 28 cases) and MALT1-negative carcinomas (83.3%; 20 of 24 cases), and the frequency of microsatellite stability increased in well-differentiated carcinomas (71.4%; 10 of 14 cases) and MALT1-positive carcinomas (77.8%; 14 of 18 cases; Fig. 2*D*). An additional microsatellite marker in the vicinity (D18S1117) had MSI limited to two cases, indicating that the genetic instability at the *MALT1* locus is selective.

Because MSI is closely associated with gene silencing through promoter methylation (19, 21), the methylation status of the *MALT1* promoter CpG island (−13 to −341 from the transcription start site) was investigated in carcinoma cell lines with different *MALT1* expression levels (Fig. 3*A*). Although the CpG island contains 37 methylation-susceptible cytosines, bisulfite-modified genomic sequencing detected methylation specifically at $^{-256}$C and not at other cytosines (Supplementary Fig. S3). Then, MSP was performed on carcinoma cells isolated from tissue sections (n = 20). The methylation was preferentially detected in MALT1-negative and MSI carcinomas (Fig. 3*B*). MSP analyses of carcinoma cell lines confirmed the correlation between $^{-256}$C methylation and *MALT1* expression (Fig. 3*C*). The 5-aza-2-deoxycytidine demethylation treatment of *MALT1* promoter–methylated cell lines (HSC2 cells and SCCKN cells) up-regulated *MALT1* expression, but unmethylated cell lines (Ho1N1 cells and KOSC2 cell) did not respond to the treatment (Fig. 3*D*). These data indicate that the specific cytosine methylation at −256 is responsible for the loss of MALT1 expression.

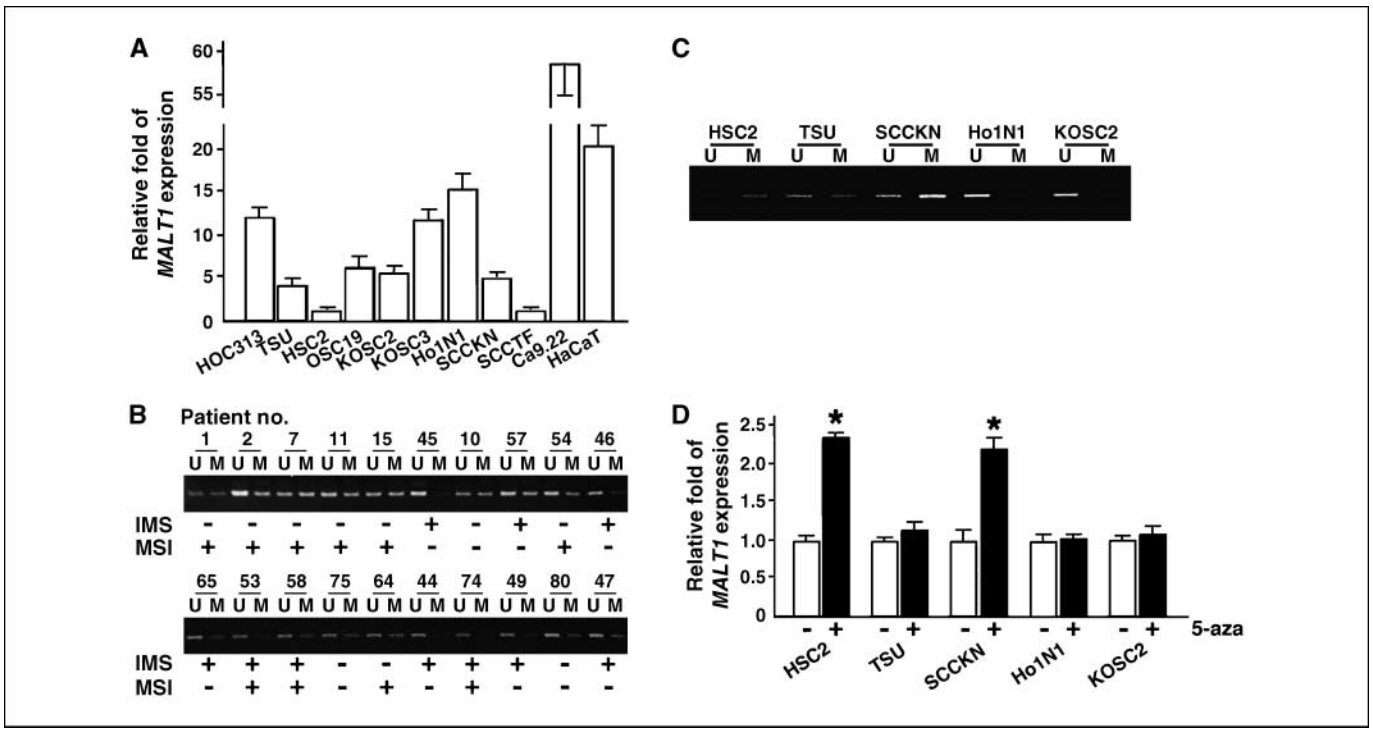

Figure 3. Methylation of *MALT1* promoter cytosine. *A,* expression of *MALT1* mRNA in oral carcinoma cell lines and normal keratinocytes (HaCaT). *MALT1* expression was quantitatively examined by the real-time PCR. Relative expression was standardized by the expression levels of *GAPDH* in each sample (n = 3). *B,* methylation at $^{-256}$C of *MALT1* promoter in carcinomas. MSP using primer sets discriminating methylated (*M*) and unmethylated (*U*) at $^{-256}$C was performed with bisulfite-modified genomic DNA extracted from carcinoma tissue sections. *IMS,* MALT1 immunostaining positive (+) or negative (−) cases. *MSI,* presence (+) or absence (−) of MSI at the *MALT1* locus. *C,* methylation at $^{-256}$C of *MALT1* promoter in carcinoma cell lines. Methylation at $^{-256}$C was examined by MSP. *D, MALT1* mRNA expression in carcinoma cell lines with and without demethylation treatment. Total RNA was isolated from cells with (+) and without (−) 5-aza-2-deoxycytidine (*5-aza*) treatment and was subjected to quantitative real-time PCR. *Columns,* means of four samples in each cell line; *bars,* SD. *, $P < 0.001$.

Published OnlineFirst September 8, 2009; DOI: 10.1158/0008-5472.CAN-09-1140

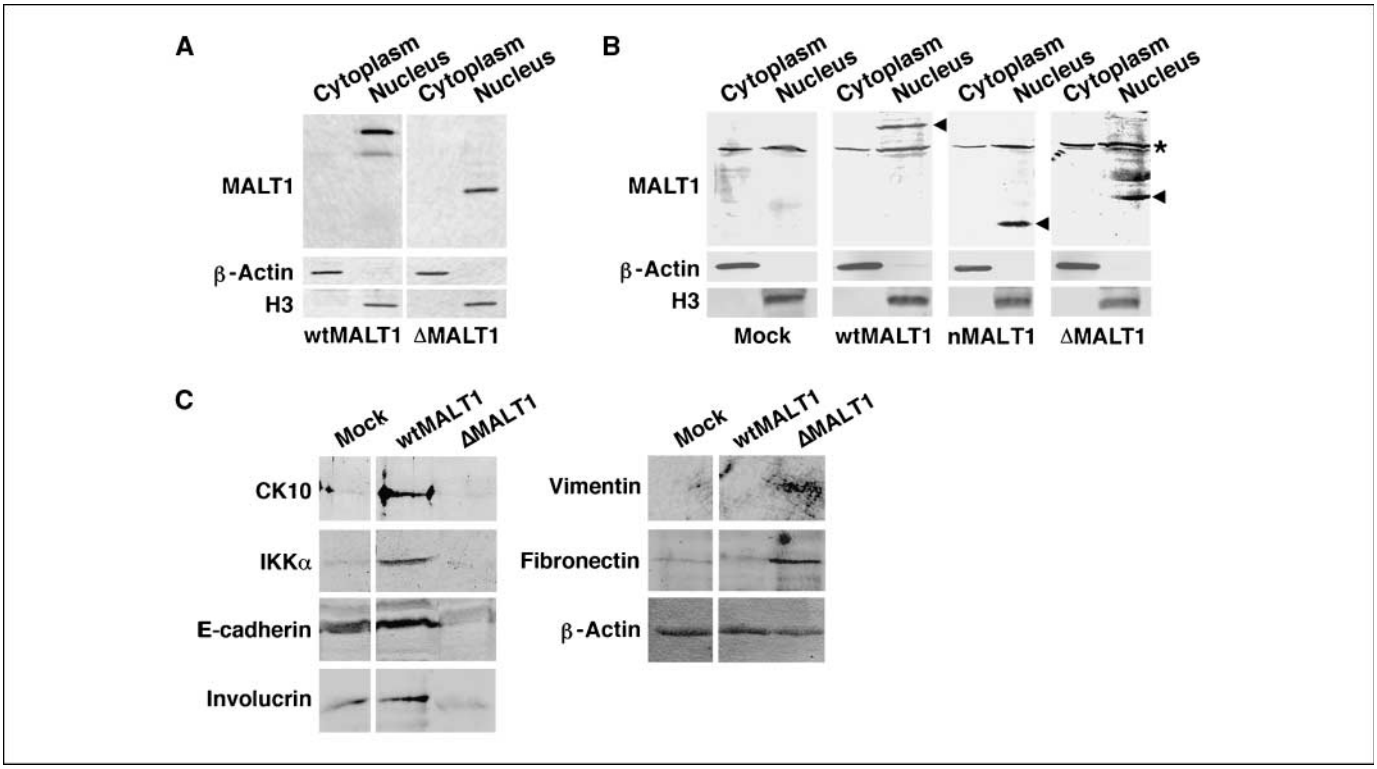

Figure 4. Nuclear localization of MALT1 protein and NF-κB activation. *A,* nuclear localization of MALT1 protein in MALT1 stably expressing HSC2 cells. Western blot shows localization of MALT1 in the nucleus, but not in the cytoplasmic fraction. β-Actin and histone H3 were loaded as markers for cytoplasmic and nuclear fractions, respectively. *B,* nuclear localization of transiently transfected MALT1 constructs. The wtMALT1, nMALT1, or ΔMALT1 proteins were detected in the nuclear fractions of HSC2 cells by immunoblotting (*arrowheads*). *, nonspecific bands. *C,* total cell lysates of HSC2 cells stably expressing *wtMALT1, ΔMALT1*, or vector alone (*mock*) were subjected to immunoblotting for keratinocyte differentiation markers (CK10, IKKα, E-cadherin, and involucrin) and mesenchymal cell-type markers (vimentin and fibronectin). β-Actin was used as an internal control. *CK10,* cytokeratin 10; and *IKKα,* IκB kinase-α.

Nuclear localization of MALT1. The abovementioned findings strongly suggest that MALT1 localizes within the nucleus and that the epigenetic loss of expression is associated with the progression of oral carcinomas. Because MALT1 is characterized as a cytoplasmic signaling molecule (19), its domain responsible for nuclear localization in oral carcinoma cells was examined. HSC2 cells were used, which express negligible amounts of endogenous *MALT1*, and we established $_{wtMALT1}$HSC2 cells, $_{\Delta MALT1}$HSC2 cells, and $_{mock}$HSC2 cells. The wtMALT1 and ΔMALT1 proteins were expressed at comparable levels, and they were present in the nuclear fraction but not in the cytoplasmic fraction (Fig. 4*A*). Transiently transfected wtMALT1, nMALT1, and ΔMALT1 in HSC2 cells were also exclusively present in the nucleus, as previously reported (Fig. 4*B*; ref. 22), indicating that no specific domain is responsible for the nuclear localization.

Induction of EMT. Because MALT1 expression is prominently lost in carcinoma cells at the invasive front, where carcinoma cells gain the EMT phenotype (12), the expression of keratinocyte differentiation and mesenchymal cell-type markers were examined (Fig. 4*C*). The expression of differentiation markers (cytokeratin 10, IKKα, E-cadherin, and involucrin) was up-regulated in $_{wtMALT1}$HSC2 cells, whereas mesenchymal cell-type markers (vimentin and fibronectin) were up-regulated in $_{\Delta MALT1}$HSC2 cells, indicating that the loss of expression results in EMT.

Discussion

The present study shows that epigenetic loss of MALT1 expression is closely associated with the progression of oral carcinomas. MALT1 staining in the nucleus was lost in 45.0% of carcinomas with advanced clinical stages and less differentiation, as well as in patients who died of disease recurrence. Patients with loss of MALT1 expression showed the worst prognosis, and the loss of expression was an independent risk factor for patient survival. MALT1-negative carcinomas exhibited genetic instability, with the expression epigenetically inactivated by a specific cytosine methylation at −256 in the promoter. The expression of the dominant-negative form of MALT1 (ΔMALT1) induced EMT of carcinoma cells. Because chromosome 18q21.31 encodes the yet unknown tumor suppressor gene (7, 8), the present data suggest that MALT1 negatively regulates oral carcinoma progression.

Although MALT1 is known to activate NF-κB in lymphocyte lineages (9), it is also expressed in other cell types (12, 20), suggesting the possibility that it has unknown roles in different cell types. Unexpectedly, MALT1 was localized in the nucleus but not the cytoplasm of normal oral epithelial and carcinoma cells. The exclusive nuclear localization was confirmed by immunoblotting using HSC2 cells, which stably or transiently express MALT1. Although the mechanism of nuclear localization is not currently known, MALT1 binds to HSC70 (23), which shuttles binding proteins to the nucleus and may associate with keratinocyte differentiation (24, 25). We confirmed a previous study (22), which found that both the NH_2 terminus (death and Ig-like domains) and the COOH terminus (caspase-like domain) exist independently in the nucleus. Because MALT1 was localized in the nucleus of normal oral epithelial cells and MALT1-BCL10 complexes were not

Published OnlineFirst September 8, 2009; DOI: 10.1158/0008-5472.CAN-09-1140

exported into the cytoplasm in oral carcinoma cells,[5] unknown mechanism(s) to retain MALT1 in the nucleus may exist in keratinocyte lineages.

The expression pattern of MALT1 in carcinoma tissues was evaluated by immunostaining. The loss of staining was closely associated with clinical stage, tumor recurrence, and long-term patient survival rate independent of other risk factors. The loss of staining was observed in carcinoma cells at the invasive front. Carcinoma cells at the invasive front can lose their epithelial characteristics and express a set of genes typified in mesenchymal cells (11, 12, 26, 27). In this study, keratinocyte differentiation markers (cytokeratin 10, IKKα, E-cadherin, and involucrin) and mesenchymal cell type markers (vimentin and fibronectin) were up-regulated by wtMALT1 and ΔMALT1, respectively, indicating that loss of MALT1 expression induces EMT. Induction of EMT in squamous carcinoma cells drives tumor progression through the enhancement of migratory, invasive, and metastatic features (28, 29). These data strongly suggest that MALT1 staining predicts tumor aggressiveness and stratifies patients into risk groups and that the loss of expression results in EMT induction, which accounts for the transition to a more advanced stage of oral carcinoma.

Immunostaining data also indicate that the loss of expression does not occur at an early stage of carcinogenesis. This was examined with the perspective of genetic instability and promoter methylation, and it was found that MALT1-negative carcinomas frequently associate with genetic instability at the locus and $^{-256}$C methylation in its promoter. MSI itself arises through defective DNA mismatch repair genes, which exhibit allelic imbalance in 80% of head and neck carcinomas (30) and are closely associated with gene silencing through promoter methylation (19, 31). Recent studies indicated that MSI and aberrant promoter methylation occurr selectively but not randomly at specific susceptible sites, resulting in a functional impact on the progression of tumors (32). Because MSI at the close proximity to the *MALT1* locus (D18S1117) was observed at a low frequency (two cases, 4.3%), genetic instability at the *MALT1* locus may be a selective phenomenon. Cytosine methylation responsible for the epigenetic gene inactivation is often distributed throughout the CpG islands of tumor-suppressor genes (18). However, up-regulation of *MALT1* expression by demethylation treatment in carcinoma cells with $^{-256}$C methylation indicates that methylation at the specific cytosine results in the loss of *MALT1* gene expression, as previously described for other tumor-associated genes (33–35). Although computational algorithms found no known transcription factor–binding sites at this position, it is possible that the methylation disturbs the accessibility of a transcription factor through architectural impediment of transcription unit formation. It is also interesting to note that sustained induction of EMT is responsible for *de novo* methylation at the *CDH1* (E-cadherin gene) promoter (36) and that the loss of MALT1 expression results from this methylation and induces EMT. The mechanism and role of MALT1 expression loss during carcinoma progression may exist in the intricate cellular system.

Although *MALT1*$^{-/-}$ mice are viable and fertile without any gross abnormalities, the mice are defective with regard to NF-κB activation in T and B cells (37, 38). The lack of NF-κB activation in these cell types was also noted in *BCL10* or *CARMA1* knockout mice (39, 40), indicating a critical role of the CBM complex in T-cell receptor– or B-cell receptor–mediated pathways. However, genetic ablation of NF-κB p65 and c-REL subunits decreases proliferation of epidermal cells (41), and enhanced activation of NF-κB containing p65 subunit is closely associated with the progression of squamous cell carcinomas and poor patient prognosis (42–44). These data suggest that MALT1 is functionally redundant in development or plays a role other than NF-κB activation in keratinocytes and carcinoma cells. The present study shows that MALT1 is expressed in the nucleus of oral epithelial cells and has epigenetically inactivated its expression in parallel with tumor progression. MALT1 immunostaining could be a prognostic determinant for stratifying patients into risk groups. Understanding the role of the loss of MALT1 expression in the pathology of oral carcinomas may provide a novel strategy for cancer therapy.

Disclosure of Potential Conflicts of Interest

No potential conflicts of interest were disclosed.

Acknowledgments

Received 3/27/09; revised 7/12/09; accepted 7/14/09; published OnlineFirst 9/8/09.

Grant support: Uehara Memorial Foundation and the Japan Society for the Promotion of Science #18592073 (K. Imai).

The costs of publication of this article were defrayed in part by the payment of page charges. This article must therefore be hereby marked *advertisement* in accordance with 18 U.S.C. Section 1734 solely to indicate this fact.

We thank Dr. M. Seto (Aichi Cancer Center) for providing MALT1 and BCL10 cDNAs and Drs. K. Chada (UMDNJ) and J. D'Armiento (Columbia University) for critical reading of the manuscript.

[5] T. Chiba, et al., manuscript in preparation.

References

1. Choi S, Myers JN. Molecular pathogenesis of oral squamous cell carcinoma: implications for therapy. J Dent Res 2008;87:14–32.
2. Pearlstein RP, Benninger MS, Carey TE, et al. Loss of 18q predicts poor survival of patients with squamous cell carcinoma of the head and neck. Genes Chromosomes Cancer 1998;21:333–9.
3. Takebayashi S, Hickson A, Ogawa T, et al. Loss of chromosome arm 18q with tumor progression in head and neck squamous cancer. Genes Chromosomes Cancer 2004;41:145–54.
4. Hidaka S, Yasutake T, Kondo M, et al. Frequent gains of 20q and losses of 18q are associated with lymph node metastasis in intestinal-type gastric cancer. Anticancer Res 2003;23:3353–7.
5. Yin Z, Babaian RJ, Troncoso P, et al. Limiting the location of putative human prostate cancer tumor suppressor genes on chromosome 18q. Oncogene 2001;20:2273–80.
6. Tenesa A, Farrington SM, Prendergast JG, et al. Genome-wide association scan identifies a colorectal cancer susceptibility locus on 11q23 and replicates risk loci at 8q24 and 18q21. Nat Genet 2008;40:631–7.
7. Takebayashi S, Ogawa T, Jung KY, et al. Identification of new minimally lost regions on 18q in head and neck squamous cell carcinoma. Cancer Res 2000;60:3397–403.
8. Blons H, Laccourreye O, Houllier AM, et al. Delineation and candidate gene mutation screening of the 18q22 minimal region of deletion in head and neck squamous cell carcinoma. Oncogene 2002;21:5016–23.
9. Thome M. Multifunctional roles of MALT1 in T-cell activation. Nat Rev Immunol 2008;8:495–500.
10. McAllister-Lucas LM, Ruland J, Siu K, et al. CARMA1/Bcl10/MALT1-dependent NF-κB activation mediates angiotensin II-responsive inflammatory signaling in nonimmune cells. Proc Natl Acad Sci U S A 2007;104:139–44.
11. Mizunuma H, Miyazawa J, Sanada K, Imai K. The LIM-only protein, LMO4, and the LIM domain-binding protein, LDB1, expression in squamous cell carcinomas of the oral cavity. Br J Cancer 2003;88:1543–8.
12. Miyazawa J, Mitoro A, Kawashiri S, Chada KK, Imai K. Expression of mesenchyme-specific gene HMGA2 in squamous cell carcinomas of the oral cavity. Cancer Res 2004;64:2024–9.
13. Che T, You Y, Wang D, Tanner MJ, Dixit VM, Lin X. MALT1/paracaspase is a signaling component downstream of CARMA1 and mediates T cell receptor-induced NF-κB activation. J Biol Chem 2004;279:15870–6.

14. Tanaka I, Morikawa M, Okuse T, Shirakawa M, Imai K. Expression and regulation of WISP2 in rheumatoid arthritic synovium. Biochem Biophys Res Commun 2005;334:973–8.
15. International Union against Cancer. TNM classification of malignant tumors, 4th edition. Hermanek P and Solbin LH (eds). Springer-Verlag, Berlin, 1987.
16. Emmert-Buck MR, Bonner RF, Smith PD, et al. Laser capture microdissection. Science 1996;274:998–1001.
17. Choi SW, Lee KJ, Bae YA, et al. Genetic classification of colorectal cancer based on chromosomal loss and microsatellite instability predicts survival. Clin Cancer Res 2002;8:2311–22.
18. Maeda G, Chiba T, Kawashiri S, Satoh T, Imai K. Epigenetic inactivation of IκB kinase-α in oral carcinomas and tumor progression. Clin Cancer Res 2007;13:5041–7.
19. Maeda G, Chiba T, Aoba T, Imai K. Epigenetic inactivation of E-cadherin by promoter hypermethylation in oral carcinoma cells. Odontology 2007;95:24–9.
20. Klemm S, Zimmermann S, Peschel C, Mak TW, Ruland J. Bcl10 and Malt1 control lysophosphatidic acid-induced NF-κB activation and cytokine production. Proc Natl Acad Sci U S A 2007;104:134–8.
21. Ahuja N, Mohan AL, Li Q, et al. Association between CpG island methylation and microsatellite instability in colorectal cancer. Cancer Res 1997;57:3370–4.
22. Nakagawa M, Hosokawa Y, Yonezumi M, et al. MALT1 contains nuclear export signals and regulates cytoplasmic localization of BCL10. Blood 2005;106:4210–6.
23. Hosokawa Y, Suzuki H, Suzuki Y, Takahashi R, Seto M. Antiapoptotic function of apoptosis inhibitor 2-MALT1 fusion protein involved in t(11;18)(q21;q21) mucosa-associated lymphoid tissue lymphoma. Cancer Res 2004;64:3452–7.
24. Tsukahara F, Maru Y. Identification of novel nuclear export and nuclear localization-related signals in human heat shock cognate protein 70. J Biol Chem 2004;279:8867–72.
25. Boehncke WH, Dahlke A, Zollner TM, Sterry W. Differential expression of heat shock protein 70 (HSP70) and heat shock cognate protein (HSC70) in human epidermis. Arch Dermatol Res 1994;287:68–71.
26. Uraguchi M, Morikawa M, Shirakawa M, Sanada K, Imai K. Activation of WNT family expression and signaling in squamous cell carcinomas of the oral cavity. J Dent Res 2004;83:327–32.
27. Thiery JP. Epithelial-mesenchymal transitions in tumor progression. Nat Rev Cancer 2002;2:442–54.
28. Janda E, Lehmann K, Killisch I, et al. Ras and TGFβ cooperatively regulate epithelial cell plasticity and metastasis: dissection of Ras signaling pathways. J Cell Biol 2002;156:299–313.
29. Oft M, Akhurst RJ, Balmain A. Metastasis is driven by sequential elevation of H-ras and Smad2 levels. Nat Cell Biol 2002;4:487–94.
30. Nunn J, Nagini S, Risk JM, et al. Allelic imbalance at the DNA mismatch repair loci, hMSH2, hMLH1, hPMS1, hPMS2 and hMSH3, in squamous cell carcinoma of the head and neck. Oral Oncol 2003;39:115–29.
31. Nakagawa H, Nouvo GJ, Zervos EE, et al. Age-related hypermethylation of the 5′ region of MLH1 in normal colonic mucosa is associated with microsatellite-unstable colorectal cancer development. Cancer Res 2001;61:6991–5.
32. Haydon AMM, Jass JR. Emerging pathways in colorectal-cancer development. Lancet Oncol 2002;3:83–8.
33. Robertson KD, Hayward SD, Ling PD, Samid D, Ambinder RF. Transcriptional activation of the Epstein-Barr virus latency C promoter after 5-azacytidine treatment: evidence that demethylation at a single CpG site is crucial. Mol Cell Biol 1995;15:6150–9.
34. Cao YX, Jean JC, Williams MC. Cytosine methylation of an Sp1 site contributes to organ-specific and cell-specific regulation of expression of the lung epithelial gene t1 α. Biochem J 2000;350:883–90.
35. Graessmann A, Sandberg G, Guhl E, Graessmann M. Methylation of single sites within the herpes simplex virus tk coding region and the simian virus 40 T-antigen intron causes gene inactivation. Mol Cell Biol 1994;14:2004–10.
36. Dumont N, Wilson MB, Crawford YG, Reynolds PA, Sigaroudinia M, Tlsty TD. Sustained induction of epithelial to mesenchymal transition activates DNA methylation of genes silenced in basal-like breast cancers. Proc Natl Acad Sci U S A 2008;105:14867–72.
37. Ruefli-Brasse AA, French DM, Dixit VM. Regulation of NF-κB-dependent lymphocyte activation and development by paracaspase. Science 2003;302:1581–4.
38. Ruland J, Duncan GS, Elia A, et al. Bcl10 is a positive regulator of antigen receptor-induced activation of NF-κB and neural tube closure. Cell 2001;104:33–42.
39. Ruland J, Duncan GS, Wakeham A, Mak TW. Differential requirement for Malt1 in T and B cell antigen receptor signaling. Immunity 2003;19:749–58.
40. Hara H, Wada T, Bakal C, et al. The MAGUK family protein CARD11 is essential for lymphocyte activation. Immunity 2003;18:763–75.
41. Gugasyan R, Voss A, Varigos G, et al. The transcription factor c-rel and RelA control epidermal development and homeostasis in embryonic and adult skin via distinct mechanisms. Mol Cell Biol 2004;24:5733–45.
42. Ondrey FG, Dong G, Sunwoo J, et al. Constitutive activation of transcription factor NF-κB, AP-1, and NF-IL6 in human head and neck squamous cell carcinoma cell lines that express pro-inflammatory cytokine and pro-angiogenic cytokines. Mol Carcinogen 1999;26:119–29.
43. Dong G, Chen Z, Kato T, Van Waes C. The host environment promotes the constitutive activation of nuclear factor-κB and proinflammatory cytokine expression during metastatic tumor progression of murine squamous cell carcinoma. Cancer Res 1999;59:3495–504.
44. Zhang PL, Pellitteri PK, Law A, et al. Overexpression of phosphorylated nuclear factor-κB in tonsillar squamous cell carcinoma and high-grade dysplasia is associated with poor prognosis. Mod Pathol 2005;18:924–32.

Cancer Research
The Journal of Cancer Research (1916–1930) | The American Journal of Cancer (1931–1940)

AACR American Association for Cancer Research

Epigenetic Loss of Mucosa-Associated Lymphoid Tissue 1 Expression in Patients with Oral Carcinomas

Tadashige Chiba, Genta Maeda, Shuichi Kawashiri, et al.

Cancer Res 2009;69:7216-7223. Published OnlineFirst September 8, 2009.